PROCEEDINGS A

rspa.royalsocietypublishing.org

Research

Cite this article: Xin F, Lu TJ. 2018 Acousto-thermo-mechanical deformation of hydrogels coupled with chemical diffusion. *Proc. R. Soc. A* **474**: 20180293. http://dx.doi.org/10.1098/rspa.2018.0293

Received: 3 May 2018
Accepted: 17 August 2018

Subject Areas:
mechanical engineering, mathematical modelling, acoustics

Keywords:
acousto-thermo-mechanical deformation, hydrogels, chemical diffusion

Author for correspondence:
Fengxian Xin
e-mail: fengxian.xin@gmail.com

Electronic supplementary material is available online at rs.figshare.com.

THE ROYAL SOCIETY PUBLISHING

Acousto-thermo-mechanical deformation of hydrogels coupled with chemical diffusion

Fengxian Xin[1,2] and Tian Jian Lu[1,2]

[1]State Key Laboratory for Strength and Vibration of Mechanical Structures, and [2]MOE Key Laboratory for Multifunctional Materials and Structures, Xi'an Jiaotong University, Xi'an 710049, People's Republic of China

FX, 0000-0001-8855-5366

We develop an acousto-thermo-mechanical theory for nonlinear (large) deformation of temperature-sensitive hydrogels subjected to temperature and ultrasonic inputs, with diffusion mass transport driven by osmotic pressure accounted for. On the basis of the strain energy due to network stretching, the mixing energy of polymers and small molecules, the Cauchy stress of the deformed hydrogel can be obtained. The acoustic radiation stress generated by the ultrasonic inputs is incorporated into the Cauchy stress to give the constitutive equations of the acousto-thermal-mechanical hydrogel. The mixing energy contains an interaction parameter as a function of temperature and polymer concentration so that hydrogel deformation is temperature dependent. By employing the incompressible condition of polymers and molecules, both the temperature and acoustic radiation stress contribute to osmotic pressure, inducing hydrogel swelling (or shrinking). Specifically, for a temperature-sensitive hydrogel layer immersed in solvent, its acoustic-triggered large deformation is comprehensively analysed under different boundary conditions (e.g. free swelling, uniaxial constraint and biaxial constraint).

1. Introduction

Polymer gels consisted of cross-linked polymer networks in three-dimensional (3D) configurations can undergo large reversible shape transformation in response to various stimuli, such as mechanical force, temperature,

pH values, acoustic, light and electric field [1–9]. Under such external stimuli, the change of osmotic pressure can drive solvent molecules to move in or out of the gel, resulting in swelling or shrinking deformation, attractive for applications in biomedical devices, optical devices, microfluidic devices, soft robotics and so like [10–13]. To facilitate more applications of gels in these fields, an acousto-thermo-mechanical theory for the reversible deformation of temperature-sensitive hydrogels coupled with chemical diffusion is developed in this study. The theory is then used to analyse specified deformation behaviours of gel under different conditions such as free swelling, uniaxial constraint and biaxial constraint.

Great efforts have been devoted to establishing theories for the large reversible deformation behaviour of stimuli-responsive polymer gels under various external loads. As a pioneer, Gibbs [14] developed a theory for the large deformation of elastic solids coupled with fluid transport. Coupled with Darcy's law for creeping fluid flow and assuming small deformation, Biot established a linear poroelasticity theory for soil consolidation to account for the effect of fluid transport on solid deformation [15,16]. By introducing a friction coefficient, Tanaka & Fillmore formulated a linear diffusion equation to consider fluid–structure interaction [17]. With pore pressure taken as a variable, Scherer [18] treated the gel as a continuum solid to develop a homogenization theory. On the basis of polymer gel thermodynamics, a number of field theories were developed to model the large deformation of gel coupled with mass transport. For instance, based on the balance of a continuum with mass diffusion, Baek & Srinivasa [19] developed a model for a swelling solid undergoing large deformation coupled with slow diffusion of a fluid. In the framework of thermodynamics, Hong *et al*. [20] established a field theory for the large deformation of polymer gels coupled with mass transport. Marcombe *et al*. [21] presented a theory of constrained swelling of a pH-sensitive hydrogel. Adopting the Flory–Rehner model, Cai & Suo [22] theoretically investigated the phase transition of temperature-sensitive hydrogels under mechanical and temperature loads. Recently, we proposed an acoustomechanical theory of polymer gels by combining the acoustic radiation stress theory and the nonlinear elasticity theory, with strong interaction between deformed configuration and wave propagation accounted for [9].

The large deformation behaviour of temperature-responsive hydrogels has been extensively studied and harnessed to design thermal driven actuators [2,3,23]. Moreover, it has been experimentally demonstrated that acoustic radiation stress can be sufficiently large to induce large deformation in soft materials [24–30]. (Here, completely different from acoustic pressure, the acoustic radiation stress is induced by the nonlinearity and interface mismatch of acoustic wave and scales as the second-order of acoustic field.) To accurately describe the acoustic-triggered deformation, the acoustomechanical constitutive theory [31] for soft materials was first proposed, upon which the deformation [32–34] and stability [35] behaviours of soft materials were then analysed in details. Further considering the diffusion effect, a nonlinear acoustomechanical field theory [9] was developed to study the acoustomechanical deformation of polymeric gels. However, at present, for temperature-responsive hydrogels, the reversible deformation of the hydrogels under combined acoustic inputs and thermal load remains elusive. This urgently needs an acousto-thermo-mechanically coupled theory for the reversible deformation of the hydrogels. Given that the ultrasonic inputs can trigger gel deformation in a fast and non-contact manner, such a theory can provide a useful guideline for designing acousto-thermally driven actuators made of temperature-sensitive hydrogels.

This article is organized as follows. The acousto-thermo-mechanically coupled theory for temperature-sensitive hydrogels is developed in §2 by using the combined free energy of polymer gel, which contains the strain energy of the network, the mixing energy of the polymer and solvent, as well as the negative work done by acoustic radiation stress. The theory is validated against existing experimental measurements in §3. In §4, the variation of gel-free energy with acoustic inputs and temperature is analysed. In §5, a comprehensive calculation and discussion of acoustic-actuated large deformation are performed under three different boundary conditions (i.e. free swelling, uniaxial constraint and biaxial constraint). Concluding remarks are presented in §6.

2. Acousto-thermo-mechanics of hydrogels

We now formulate the theoretical framework of acousto-thermo-mechanics of temperature-sensitive hydrogels. The dry network with initial dimensions (L_1, L_2 and L_3) is taken as reference configuration. When the dry network is immersed in water, it imbibes water and freely swells to reach an equilibrium state with dimensions ($\lambda_0 L_1$, $\lambda_0 L_2$ and $\lambda_0 L_3$), λ_0 being the free swelling ratio. In such cases, three displacement boundary conditions can be used to design actuators for different applications. As shown in figure 1*a–c*, the hydrogel can be designed to be free swelling, subjected to uniaxial constraint and biaxial constraint, respectively. When the hydrogel is subjected further to ultrasonic inputs and temperature environment, material particle $\mathbf{X}$ in reference configuration moves to $\mathbf{x}$ in current configuration. The deformation gradient $\mathbf{F} = \partial \boldsymbol{x}/\partial \mathbf{X}$ describes the deformation kinematics of the polymer network from reference to current configuration. The Cauchy stress is related to the first Piola-Kirchhoff stress as $\boldsymbol{\sigma} = \mathbf{s} \cdot \mathbf{F}^{\mathrm{T}}/\det(\mathbf{F})$.

For the free swelling and uniaxial constraint cases, we exert two counterpropagating ultrasonic inputs having identical amplitude, frequency and phase position. The propagation of ultrasonic waves in the medium generates acoustic radiation stress. The two counterpropagating acoustic fields are symmetric with respect to the midplane of the hydrogel layer and thereby the hydrogel undergoes large deformation but does not move. By contrast, for the biaxial constraint case, only one ultrasonic input is applied from the water side because the hydrogel is bonded to a rigid substrate on the other side. As the ultrasonic wave penetrates through the hydrogel and totally reflects at the interface between the hydrogel and the rigid substrate, it will still give rise to two counterpropagating acoustic fields. In addition, it is assumed that the in-plane dimensions of the hydrogel layer are much larger than its thickness so that it can be regarded as only undergoing homogeneous deformation with principal stretches (λ_1, λ_2 and λ_3).

To establish a comprehensive theory of hydrogel acousto-thermo-mechanics, we consider a temperature-sensitive hydrogel subjected to combined acoustic radiation force and temperature load. To this end, we first recall the nonlinear elastic theory of hydrogel thermo-mechanics. The free energy of hydrogel thermo-mechanics contains contributions from stretching the network, mixing the polymer and solvent, as:

$$W(\mathbf{F}, C) = W_{\mathrm{e}}(\mathbf{F}) + W_{\mathrm{m}}(C), \tag{2.1}$$

where $\mathbf{F} = \partial \mathbf{x}/\partial \mathbf{X}$ is the deformation gradient and C is the nominal solvent concentration (i.e. number of solvent molecules per unit volume of hydrogel). Following the Flory–Rehner model, the free energy related to network stretching is:

$$W_{\mathrm{e}}(\mathbf{F}) = \frac{1}{2} NkT(I_1 - 3 - 2\ln J), \tag{2.2}$$

where $I_1 = \mathrm{tr}(\mathbf{F}^{\mathrm{T}}\mathbf{F})$, $J = \det(\mathbf{F})$, N is the effective number of polymer chains per unit volume of polymer, k is the Boltzmann constant and T is the absolute temperature. With the effect of cross-links on solution ignored as an approximation, the free energy of mixing the polymers and solvent may be given as:

$$W_{\mathrm{m}}(C) = \frac{kT}{\Omega}\left[\Omega C \ln\left(\frac{\Omega C}{1+\Omega C}\right) + \frac{\chi \Omega C}{1+\Omega C}\right], \tag{2.3}$$

where Ω is the volume per solvent molecule and χ is the Flory interaction parameter. Traditionally, the Flory interaction parameter in the Flory–Rehner model is often taken as a temperature-independent constant. In practice, however, the Flory interaction parameter may have non-trivial dependence on polymer fraction and temperature, especially for temperature-sensitive hydrogels [36]. In such cases, the Flory interaction parameter can be written as the first-order Taylor expansion of the volume fraction φ of polymer in the hydrogel:

$$\chi = \chi_0 + \chi_1 \varphi, \tag{2.4}$$

with

$$\chi_0 = A_0 + B_0 T, \quad \chi_1 = A_1 + B_1 T, \quad \varphi = \frac{1}{1+\Omega C}. \tag{2.5}$$

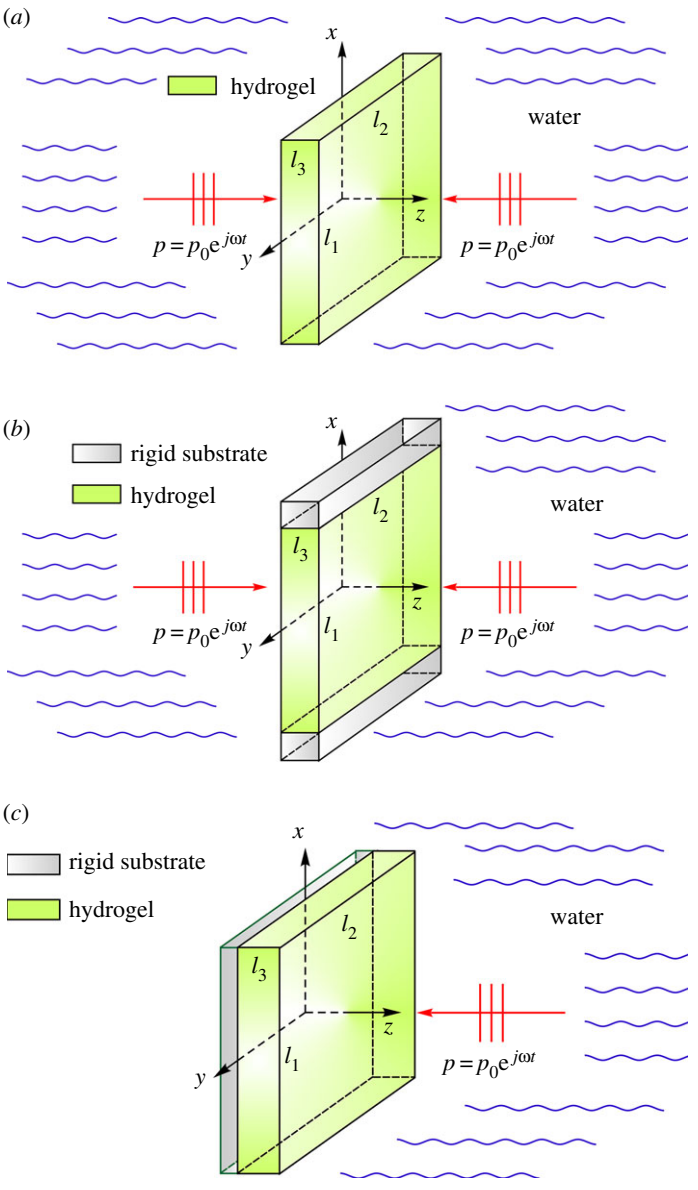

Figure 1. A temperature-sensitive hydrogel layer with different boundary conditions is immersed in water, which deforms in response to acoustic inputs and temperature environment: (*a*) free swelling with two counterpropagating acoustic inputs; (*b*) uniaxial constraint with two counterpropagating acoustic inputs and (*c*) biaxial constraint with one acoustic input.

For PNIPAM hydrogel, the values of A_0, B_0, A_1 and B_1 have been experimentally determined [37] as $A_0 = -12.947$, $B_0 = 0.04496$, $A_1 = 17.92$ and $B_1 = -0.0569$, which will be adopted in this study to perform numerical calculations.

The molecule incompressible condition dictates that:

$$1 + \Omega C = \det(\mathbf{F}) = J. \tag{2.6}$$

Upon substituting equations (2.4)–(2.6) into equation (2.3), the mixing free energy can be re-written as:

$$W_m(\mathbf{F}) = \frac{kT}{\Omega}\left[(J-1)\ln\left(1-\frac{1}{J}\right) + \left(\chi_0 + \frac{\chi_1}{J}\right)\left(1-\frac{1}{J}\right)\right]. \tag{2.7}$$

Combining the two contributions yields the total free energy of the thermo-mechanical hydrogel at given temperature T. The total free energy can thence be expressed as a function of deformation gradient, as:

$$W(\mathbf{F}) = \frac{1}{2}NkT(I_1 - 3 - 2\ln J) + \frac{kT}{\Omega}\left[(J-1)\ln\left(1-\frac{1}{J}\right) + \left(\chi_0 + \frac{\chi_1}{J}\right)\left(1-\frac{1}{J}\right)\right]. \tag{2.8}$$

With molecule incompressible condition, chemical diffusion can be introduced into the first Piola-Kirchhoff stress, as

$$\begin{aligned}\mathbf{s} &= \frac{\partial W(\mathbf{F})}{\partial \mathbf{F}} - \frac{\mu}{\Omega}J\mathbf{F}^{-\mathbf{T}} \\ &= NkT(\mathbf{F}^{\mathbf{T}} - \mathbf{F}^{-\mathbf{T}}) + \frac{kT}{\Omega}\left[\ln\left(1-\frac{1}{J}\right) + \frac{1}{J} + \frac{\chi_0 - \chi_1}{J^2} + \frac{2\chi_1}{J^3}\right]J\mathbf{F}^{-\mathbf{T}} - \frac{\mu}{\Omega}J\mathbf{F}^{-\mathbf{T}},\end{aligned} \tag{2.9}$$

where μ is the chemical potential of solvent, Ω is the volume per solvent molecule and μ/Ω actually denotes the osmotic pressure, which increases the chemical potential when the solvent diffuses into the gel. The corresponding Cauchy stress is:

$$\begin{aligned}\boldsymbol{\sigma} &= \frac{\mathbf{F}}{J}\frac{\partial W(\mathbf{F})}{\partial \mathbf{F}} - \frac{\mu}{\Omega}\mathbf{I} \\ &= \frac{NkT}{J}(\mathbf{F}\mathbf{F}^{\mathbf{T}} - \mathbf{I}) + \frac{kT}{\Omega}\left[\ln\left(1-\frac{1}{J}\right) + \frac{1}{J} + \frac{\chi_0 - \chi_1}{J^2} + \frac{2\chi_1}{J^3}\right]\mathbf{I} - \frac{\mu}{\Omega}\mathbf{I}.\end{aligned} \tag{2.10}$$

Upon the above-mentioned hydrogel thermo-mechanics, we further consider the acoustic momentum contribution to the Cauchy stress. As is known, ultrasonic wave propagation in media is accompanied by changes in energy density and momentum density flux, which produces a steady time-averaged stress called as acoustic radiation stress in the path of wave propagation. Note that, arising from acoustic momentum transfer at nonlinear acoustic levels or at discontinuous interfaces, the acoustic radiation stress is not acoustic pressure. Given the acoustic input $p(\mathbf{x},t) = p_0 e^{-j(\mathbf{k}\cdot\mathbf{x}-\omega t)}$ (here p_0 acoustic amplitude, $\mathbf{k}$ acoustic wavenumber and ω angular frequency), the velocity potential $\phi(\mathbf{x},t)$ (i.e. particle velocity $\mathbf{u} = -\nabla\phi$) of the acoustic field can be obtained on the basis of the Helmholtz equation and boundary conditions. (For more details, see electronic supplementary material, appendix A). Once the velocity potential is known, the acoustic radiation stress can be expressed as a function of velocity potential [9,31,33]:

$$\langle T_{ij}\rangle = \left[\frac{\rho_a}{2c_a^2}\left\langle\left(\frac{\partial\phi}{\partial t}\right)^2\right\rangle - \frac{\rho_a\langle(\nabla\phi)^2\rangle}{2}\right]\delta_{ij} + \rho_a\left\langle\frac{\partial\phi}{\partial x_i}\frac{\partial\phi}{\partial x_j}\right\rangle, \tag{2.11}$$

or as a function of acoustic pressure and particle velocity

$$\langle T_{ij}\rangle = \left[\frac{\langle p^2\rangle}{2\rho_a c_a^2} - \frac{\rho_a\langle u_k u_k\rangle}{2}\right]\delta_{ij} + \rho_a\langle u_i u_j\rangle, \tag{2.12}$$

where T_{ij} is the acoustic momentum flux tensor, whose time-average $\langle T_{ij}\rangle$ is the second-rank acoustic radiation stress tensor (expressed now in Eulerian coordinates) with $\langle\cdot\rangle$ being the time-average over an oscillation cycle. ρ_a is the density of medium, c_a is the acoustic phase velocity and δ_{ij} is the Kronecker delta.

To consider the contribution of acoustic momentum on the acousto-thermo-mechanical coupling hydrogel, the acoustic radiation stress can be added to the Cauchy stress

$$\begin{aligned}\boldsymbol{\sigma} &= \frac{\mathbf{F}}{J}\frac{\partial W(\mathbf{F})}{\partial \mathbf{F}} - \frac{\mu}{\Omega}\mathbf{I} - \langle\mathbf{T}\rangle \\ &= \frac{NkT}{J}(\mathbf{F}\mathbf{F}^{\mathbf{T}} - \mathbf{I}) + \frac{kT}{\Omega}\left[\ln\left(1-\frac{1}{J}\right) + \frac{1}{J} + \frac{\chi_0 - \chi_1}{J^2} + \frac{2\chi_1}{J^3}\right]\mathbf{I} - \frac{\mu}{\Omega}\mathbf{I} - \langle\mathbf{T}\rangle.\end{aligned} \tag{2.13}$$

For the considered thin film case, its deformation occurs along the three principal directions. To simplify the following analysis, the acoustic radiation stress in principal directions can be

approximately homogenized as the equivalent acoustic radiation stress (because the film is considered thin), as below

$$\left.\begin{aligned} t_1 &= \frac{1}{l_3}\int_0^{l_3} \langle T_{11}^{\text{inside}}(z)\rangle \mathrm{d}z, \\ t_2 &= \frac{1}{l_3}\int_0^{l_3} \langle T_{22}^{\text{inside}}(z)\rangle \mathrm{d}z \\ \text{and} \quad t_3 &= \langle T_{33}^{\text{inside}}(l_3)\rangle - \langle T_{33}^{\text{outside}}(l_3)\rangle, \end{aligned}\right\} \tag{2.14}$$

where T_{11}^{inside}, T_{22}^{inside} and T_{33}^{inside} is the acoustic radiation stress inside the hydrogel in the x-, y- and z-directions, respectively, while T_{33}^{outside} is the acoustic radiation stress outside the hydrogel in the z-direction. An explicit relation between these equivalent acoustic radiation stresses and the acoustic input can be found in the electronic supplementary material, appendix A. Applying the equivalent acoustic radiation stress, the principal components of Cauchy stress for the specified thin film are written as:

$$\sigma_1 = \frac{NkT}{J}(\lambda_1^2 - 1) + \frac{kT}{\Omega}\left[\ln\left(1 - \frac{1}{J}\right) + \frac{1}{J} + \frac{\chi_0 - \chi_1}{J^2} + \frac{2\chi_1}{J^3}\right] - \frac{\mu}{\Omega} - t_1, \tag{2.15}$$

$$\sigma_2 = \frac{NkT}{J}(\lambda_2^2 - 1) + \frac{kT}{\Omega}\left[\ln\left(1 - \frac{1}{J}\right) + \frac{1}{J} + \frac{\chi_0 - \chi_1}{J^2} + \frac{2\chi_1}{J^3}\right] - \frac{\mu}{\Omega} - t_2 \tag{2.16}$$

and

$$\sigma_3 = \frac{NkT}{J}(\lambda_3^2 - 1) + \frac{kT}{\Omega}\left[\ln\left(1 - \frac{1}{J}\right) + \frac{1}{J} + \frac{\chi_0 - \chi_1}{J^2} + \frac{2\chi_1}{J^3}\right] - \frac{\mu}{\Omega} - t_3. \tag{2.17}$$

As a counterpart of Cauchy stress, the first Piola-Kirchhoff stress in Lagrangian coordinates is expressed as follows:

$$\begin{aligned} \mathbf{s} &= \frac{\partial W(\mathbf{F})}{\partial \mathbf{F}} - \frac{\mu}{\Omega} J\mathbf{F}^{-\mathbf{T}} - \langle \mathbf{T}\rangle J\mathbf{F}^{-\mathbf{T}} \\ &= NkT(\mathbf{F}^{\mathbf{T}} - \mathbf{F}^{-\mathbf{T}}) + \frac{kT}{\Omega}\left[\ln\left(1 - \frac{1}{J}\right) + \frac{1}{J} + \frac{\chi_0 - \chi_1}{J^2} + \frac{2\chi_1}{J^3}\right] J\mathbf{F}^{-\mathbf{T}} - \frac{\mu}{\Omega} J\mathbf{F}^{-\mathbf{T}} - \langle \mathbf{T}\rangle J\mathbf{F}^{-\mathbf{T}}. \end{aligned} \tag{2.18}$$

In the three principal stretch directions, applying the equivalent acoustic radiation stress, the first Piola-Kirchhoff stress for the specified thin film can be written as follows:

$$s_1 = NkT(\lambda_1 - \lambda_1^{-1}) + \frac{kT}{\Omega}\left[\ln\left(1 - \frac{1}{J}\right) + \frac{1}{J} + \frac{\chi_0 - \chi_1}{J^2} + \frac{2\chi_1}{J^3}\right] J\lambda_1^{-1} - J\lambda_1^{-1}\frac{\mu}{\Omega} - J\lambda_1^{-1}t_1, \tag{2.19}$$

$$s_2 = NkT(\lambda_2 - \lambda_2^{-1}) + \frac{kT}{\Omega}\left[\ln\left(1 - \frac{1}{J}\right) + \frac{1}{J} + \frac{\chi_0 - \chi_1}{J^2} + \frac{2\chi_1}{J^3}\right] J\lambda_2^{-1} - J\lambda_2^{-1}\frac{\mu}{\Omega} - J\lambda_2^{-1}t_2 \tag{2.20}$$

and

$$s_3 = NkT(\lambda_3 - \lambda_3^{-1}) + \frac{kT}{\Omega}\left[\ln\left(1 - \frac{1}{J}\right) + \frac{1}{J} + \frac{\chi_0 - \chi_1}{J^2} + \frac{2\chi_1}{J^3}\right] J\lambda_3^{-1} - J\lambda_3^{-1}\frac{\mu}{\Omega} - J\lambda_3^{-1}t_3. \tag{2.21}$$

Apart from the above constitutive equations, the deformation of hydrogel must satisfy mechanical equilibrium at all time during the transient process, namely:

$$\frac{\partial \boldsymbol{\sigma}(\mathbf{x}, t)}{\partial \mathbf{x}} + \mathbf{f}^b(\mathbf{x}, t) = \rho\frac{\partial^2 \mathbf{u}(\mathbf{x}, t)}{\partial t^2} \quad \text{in } V(\mathbf{x}, t) \tag{2.22}$$

and

$$\boldsymbol{\sigma}(\mathbf{x}, t)\cdot\mathbf{n}(\mathbf{x}, t) = \mathbf{f}^s(\mathbf{x}, t) \quad \text{in } A(\mathbf{x}, t), \tag{2.23}$$

where $V(\mathbf{x}, t)$ and $A(\mathbf{x}, t)$ are the volume and surface area of hydrogel, $\mathbf{f}^b(\mathbf{x}, t)$ and $\mathbf{f}^s(\mathbf{x}, t)$ are the body force and surface force, $\mathbf{n}(\mathbf{x}, t)$ is the unit vector normal to the interface between two materials (positive when pointing outside) and $\mathbf{u}(\mathbf{x}, t)$ is the displacement field.

The gradient of chemical potential drives the solvent flux in or out of the hydrogel, which can be characterized using the chemical diffusion equation, as [15]

$$\mathbf{j}(\mathbf{x},t) = -\frac{cD}{kT}\frac{\partial \boldsymbol{\mu}(\mathbf{x},t)}{\partial \mathbf{x}}, \tag{2.24}$$

where $\mathbf{j}(\mathbf{x},t)$ is the number flux of solvent molecule crossing a unit area in current configuration, $\boldsymbol{\mu}(\mathbf{x},t)$ is the chemical potential of solvent, c is the concentration of small molecules in current configuration, D is the coefficient of diffusion for solvent molecules, k is the Boltzmann constant and T is the absolute temperature.

In the meantime, mass conservation dictates the following continuity equation:

$$\frac{\partial c(\mathbf{x},t)}{\partial t} + \frac{\partial \mathbf{j}(\mathbf{x},t)}{\partial \mathbf{x}} = r(\mathbf{x},t) \quad \text{in } V(\mathbf{x},t) \tag{2.25}$$

and

$$\mathbf{j}(\mathbf{x},t)\cdot\mathbf{n}(\mathbf{x},t) = i(\mathbf{x},t) \quad \text{on } A(\mathbf{x},t), \tag{2.26}$$

where $c(\mathbf{x},t)$ is the true solvent concentration, and $r(\mathbf{x},t)$ and $i(\mathbf{x},t)$ are separately the inside source and surface source generating solvent molecules, which are generally taken as zero (i.e. no source).

The above-formulated constitutive equations together with boundary condition, diffusion equation and continuity equation describe the nonlinear deformation behaviour of acousto-thermo-mechanical hydrogels at given temperature, chemical potential and acoustic inputs. Specifically, equations (2.18)–(2.21) give the constitutive relation between the first Piola-Kirchhoff stress and the stretches, while equations (2.13)–(2.17) give the constitutive relation between the Cauchy stress and the stretches. When steady deformation of hydrogel is of concern, the diffusion equation and continuity equation are spontaneously satisfied for given sufficient time. When displacement or force boundary condition is applied, the equilibrium state of hydrogel can be obtained by solving the corresponding constitutive equations. Since the hydrogel immersed in pure water is considered in this study, as illustrated in figure 1, its chemical potential will be zero in a series of equilibrium states.

3. Validation of a theoretical model

To validate the theoretical formulations, we compare our theoretical predictions with existing experimental results [38,39]. As shown in figure 2*a*,*b*, the two cases of free swelling and uniaxial constraint are considered. For either case, the temperature is plotted as a function of hydrogel volume ratio. Since the cross-link density of the hydrogel was unknown in the experiments, we adopt the cross-link density-related parameter $N\Omega$ as an adjustable parameter to fit the experimental results. For free swelling, the selection of $N\Omega = 0.0035$, 0.01 and 0.02 matches well with experimental results. For uniaxial constraint, the hydrogel is first free swelling in water to an equilibrium swelling ratio λ_p at $T = 303\,\mathrm{K}$ before displacement constraints are exerted. The hydrogel is then stretched along x-direction to a prescribed stretch ratio λ_1, which is subsequently held unchanged in this direction. The theoretical predictions with a fitting parameter of $N\Omega = 0.0014$ agree well with the experimental results for the prescribed stretches of $\lambda_1 = \lambda_p$, $2\lambda_p$ and $3\lambda_p$. For both cases in figure 2, with the increase of the temperature, the solvent moves out of the hydrogel associated with the decrease of the volume of the hydrogel. When the temperature continues to increase and all solvents move out of the hydrogel, our theoretical predictions give the asymptotic boundary line for the hydrogel volume ratio. This asymptotic boundary line just demonstrates the phase transition for the volume of the hydrogel. As a matter of fact, the experiments used here are just for the equilibrium swelling of gels in the absence of acoustic contribution, such results mainly verify the degraded model of the present acousto-thermo-mechanical model. As there are no experimental results available for the complete acousto-thermo-mechanical coupling deformation, the present validation might be a preferred choice in the current condition.

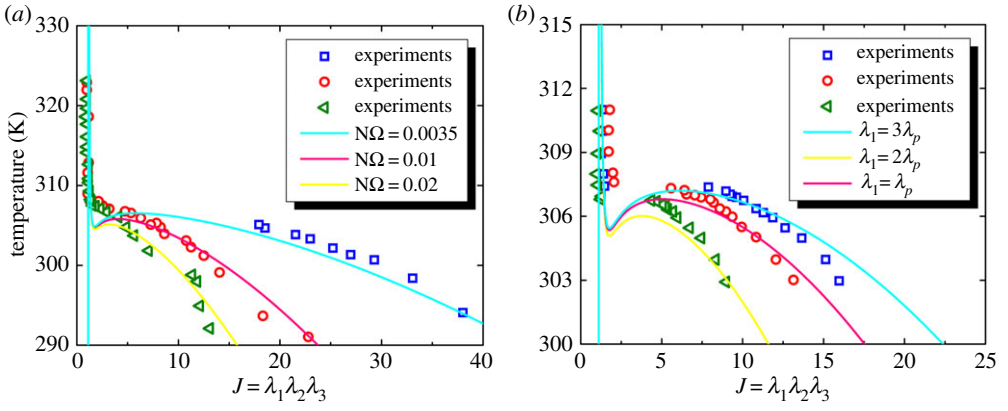

Figure 2. Comparison between theoretical predictions and experimental measurements [38,39] for temperature–volume curves of hydrogel: (*a*) free swelling and (*b*) uniaxial constraint.

4. Free energy variations

The developed acousto-thermo-mechanical theory relies on the free energy to describe the nonlinear deformation behaviour of hydrogels, which is consisted of network elastic energy, mixing energy of polymer and solvent as well as acoustical free energy (work done by acoustic radiation force). We consider next a specified case of two counterpropagating acoustic waves $p = p_0 e^{j\omega t}$ imping onto a freestanding hydrogel layer along its thickness direction. The two acoustic waves have the same amplitude p_0 and frequency ω. Figure 3 presents the effects of temperature and acoustic inputs on hydrogel-free energy.

With zero acoustic input ($(p_0^2/\rho_0 c_0^2)(\Omega/kT) = 0$, here ρ_0 and c_0 are the density and acoustic speed of the surrounding medium), figure 3*a* plots the free energy of hydrogel as a function of volume ratio for selected temperatures. At relatively large volume ratio, the temperature plays a significant role in the free energy. However, as a stable system requires minimization of its free energy, only the globally minimized free energy is related to the equilibrium state for each temperature curve. With a constant acoustic input of $(p_0^2/\rho_0 c_0^2)(\Omega/kT) = 0.015$, the variation of free energy as a function of volume ratio is shown in figure 3*b* at different temperatures. Since the acoustic radiation force is dependent upon the thickness of the hydrogel layer, the corresponding free energy exhibits a reciprocating knot at each temperature curve. Under a constant temperature of $T = 310\,\mathrm{K}$, the effect of acoustic input on free energy is displayed in figure 3*c*. The larger the acoustic input, the larger the reciprocating knot in each curve. Whatever, only the global minimization of free energy corresponds to the stable state of hydrogel: other regimes are either in the metastable or unstable states.

5. Acoustic-actuated large deformations of hydrogels

With reference to figure 1, the two counterpropagating acoustic waves along the thickness of hydrogel layer generate acoustic radiation stresses in the hydrogel and the surrounding medium (water). The difference of acoustic radiation stress across the hydrogel–water interface needs to be balanced with the network deformation stress and osmotic pressure, which can thus cause the hydrogel to undergo large deformation, either in a swollen phase or a shrunken phase. In the following sections, we consider three kinds of isotropic and homogeneous deformations of the hydrogel under different temperatures and acoustic inputs, as shown in figure 1.

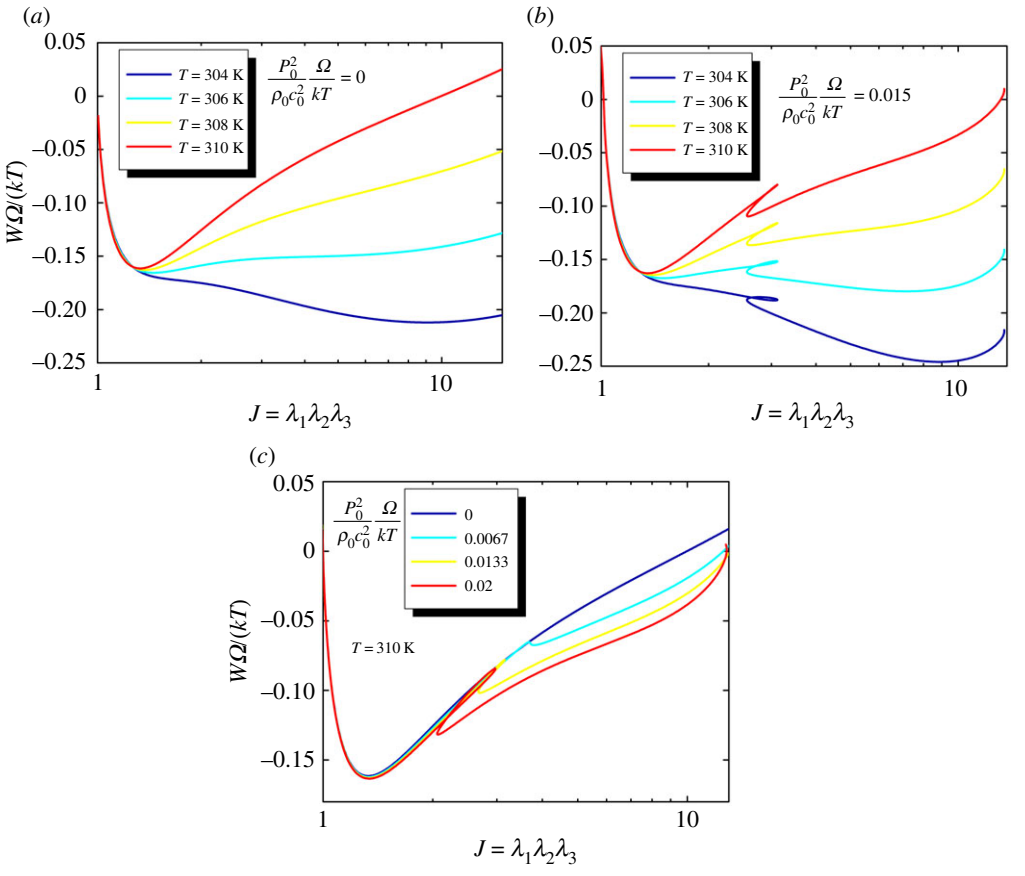

Figure 3. Equilibrium states of a freestanding hydrogel layer submerged in water: (*a*) free energy plotted as a function of volume ratio under selected temperatures without acoustic inputs; (*b*) free energy plotted as a function of volume ratio under selected temperatures with acoustic inputs and (*c*) free energy plotted as a function of volume ratio under selected acoustic inputs at fixed temperature (310 K).

(a) Free swelling

Consider a freestanding network immersed in an aqueous environment without any displacement or mechanical force constraint, which freely absorbs water and swells till reaching an equilibrium state (figure 1*a*). Subjected to the acoustic field of two counterpropagating waves input and the temperature environment, the following relations are obtained in the case of free swelling:

$$\lambda_1 = \lambda_2 \neq \lambda_3, \quad J = \lambda_1\lambda_2\lambda_3 = \lambda_1^2\lambda_3, \quad t_1 = t_2 \neq t_3, \tag{5.1}$$

$$\sigma_1 = \frac{NkT}{J}(\lambda_1^2 - 1) + \frac{kT}{\Omega}\left[\ln\left(1 - \frac{1}{J}\right) + \frac{1}{J} + \frac{\chi_0 - \chi_1}{J^2} + \frac{2\chi_1}{J^3}\right] - t_1 = 0, \tag{5.2}$$

$$\sigma_2 = \frac{NkT}{J}(\lambda_2^2 - 1) + \frac{kT}{\Omega}\left[\ln\left(1 - \frac{1}{J}\right) + \frac{1}{J} + \frac{\chi_0 - \chi_1}{J^2} + \frac{2\chi_1}{J^3}\right] - t_2 = 0 \tag{5.3}$$

and

$$\sigma_3 = \frac{NkT}{J}(\lambda_3^2 - 1) + \frac{kT}{\Omega}\left[\ln\left(1 - \frac{1}{J}\right) + \frac{1}{J} + \frac{\chi_0 - \chi_1}{J^2} + \frac{2\chi_1}{J^3}\right] - t_3 = 0. \tag{5.4}$$

From equations (5.2) and (5.4), the normalized acoustic input at a given temperature T can be expressed as:

$$\frac{p_0^2}{\rho_0 c_0^2}\frac{\Omega}{kT} = \frac{1}{t_1}\frac{p_0^2}{\rho_0 c_0^2}\left\{\frac{N\Omega}{J}(\lambda_1^2-1)+\ln\left(1-\frac{1}{J}\right)+\frac{1}{J}+\frac{1}{J^2}(A_0-A_1)+\frac{2}{J^3}A_1 + \left[\frac{1}{J^2}(B_0-B_1)+\frac{2}{J^3}B_1\right]T\right\} \tag{5.5}$$

and

$$\frac{p_0^2}{\rho_0 c_0^2}\frac{\Omega}{kT} = \frac{1}{t_3}\frac{p_0^2}{\rho_0 c_0^2}\left\{\frac{N\Omega}{J}(\lambda_3^2-1)+\ln\left(1-\frac{1}{J}\right)+\frac{1}{J}+\frac{1}{J^2}(A_0-A_1)+\frac{2}{J^3}A_1 + \left[\frac{1}{J^2}(B_0-B_1)+\frac{2}{J^3}B_1\right]T\right\}, \tag{5.6}$$

where p_0 is the amplitude of acoustic input, ρ_0 and c_0 are the density and acoustic speed of the surrounding medium. Note that the term $p_0^2/(\rho_0 c_0^2)$ is kept on both sides of the above equations, the term on the left side represents the acoustic radiation stress and also contains the original information of the acoustic input, while the term on the right side is to normalize t_1. As a matter of fact, all the details for acoustic wave propagation and the acoustic radiation stress are included in the calculation of t_1 (or t_3) (see details in electronic supplementary material, appendix A). Or in other words, the term $p_0^2/(\rho_0 c_0^2)$ that contains the information of the acoustic radiation stress and the original acoustic input is extracted from t_1 (or t_3) and moved to the left side of the equation. The residual term $p_0^2/(t_1\rho_0 c_0^2)$ (or $p_0^2/(t_3\rho_0 c_0^2)$) on the right side of the equation only contains the influence of the dimensions or deformation of the film on the acoustic wave propagation and the generation of the acoustic radiation stress. The stretch λ_1 can be expressed in terms of stretch λ_3 as:

$$\lambda_1 = \lambda_3 \Big/ \sqrt{1-\frac{(t_1-t_3)}{NkT}\lambda_3}. \tag{5.7}$$

Equations (5.5) and (5.6) give the normalized acoustic input under a given temperature. Alternatively, the temperature can be expressed as a function of hydrogel volume ratio at a given acoustic input, as:

$$T = \left\{\frac{t_3\Omega}{kT} - \left[\frac{N\Omega}{J}(\lambda_3^2-1)+\ln\left(1-\frac{1}{J}\right)+\frac{1}{J}+\frac{1}{J^2}(A_0-A_1)+\frac{2}{J^3}A_1\right]\right\}\left[\frac{1}{J^2}(B_0-B_1)+\frac{2}{J^3}B_1\right]^{-1}. \tag{5.8}$$

Figure 4*a*,*b* plots separately the normalized acoustic input as a function of stretch and volume ratio at different temperature environments, showing a series of equilibrium state for the hydrogel. In the absence of acoustic input, the hydrogel starts to deform from the free swelling ratio point, i.e. the interaction point of the curve with the zero acoustic input line. As the deformation is increased, the acoustic input first increases and then decreases after reaching a peak. Such variation trend represents snap-through instability and phase transition, that is, the hydrogel undergoes a discontinuous jumping deformation from one metastable state to another metastable state having much larger deformation. As the high temperature tends to shrink the hydrogel, larger acoustic input is needed to maintain the same stretch level when the hydrogel is immersed in a relatively high-temperature aqueous environment, as demonstrated in figure 4*a*,*b*.

The variation of temperature as a function of hydrogel stretch and volume ratio for selected acoustic inputs is plotted in figure 5*a*,*b*, respectively. At zero acoustic input, the variation of temperature with deformation is completely in agreement with existing experimental and theoretical results (figure 2), that is, the hydrogel response to temperature undergoes a discontinuous deformation jumping over the unstable region. In the presence of acoustic input, the variation of the curves in figure 5 exhibits more complex trends, because the acoustic radiation

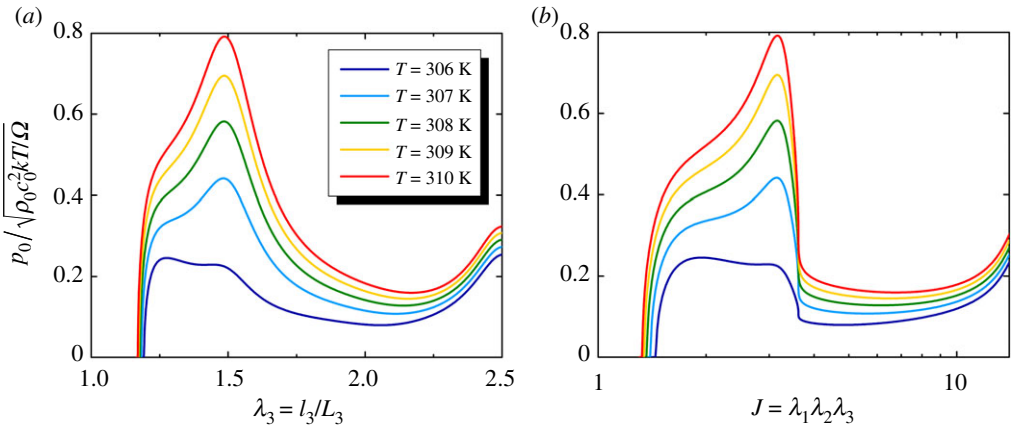

Figure 4. Nonlinear acousto-thermo-mechanical deformation of a freestanding hydrogel layer under different temperatures: (*a*) acoustic input plotted as a function of out-of-plane stretch λ_3 and (*b*) acoustic input plotted as a function of volume ratio.

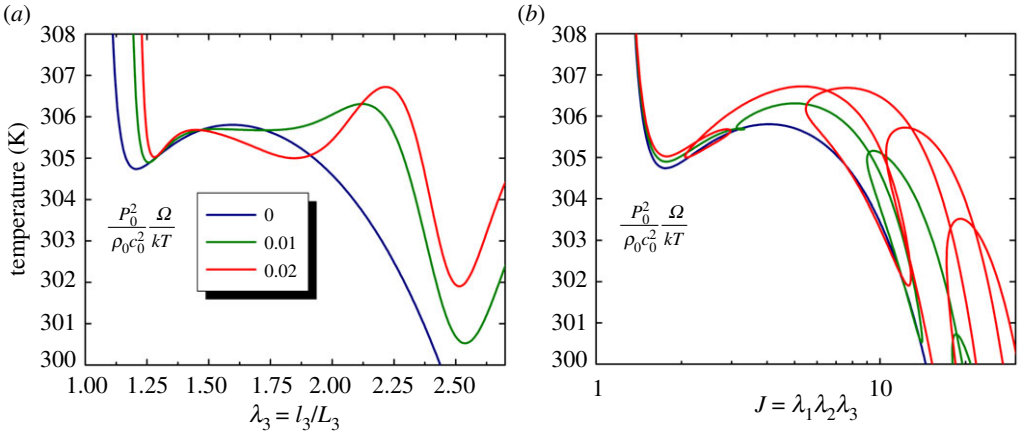

Figure 5. Nonlinear thermo-acousto-mechanical deformation of a freestanding hydrogel layer at prescribed acoustic inputs: (*a*) temperature plotted as a function of out-of-plane stretch and (*b*) temperature plotted as a function of volume ratio.

force is a quasi-periodic function of hydrogel thickness, thus sensitive to hydrogel geometry. The acoustic radiation force plays a role by superposing its quasi-periodic variation on the curve related to zero acoustic input. Relative to the wavy variation of the curves in figure 5*a*, the temperature variation with hydrogel volume exhibits a series of reciprocating knots, because the volume ratio is a nonlinear function of the stretch. As the acoustic input is increased, the reciprocating knots tend to appear at smaller volume ratios, demonstrating the increasing influence of acoustic radiation force.

(b) Uniaxial constraint

We further consider a temperature-sensitive hydrogel with uniaxial constraint, as shown in figure 1*b*. The hydrogel layer is first put into water at $T = 303\,\mathrm{K}$, freely swells to reach an equilibrium state with a swelling ratio λ_p and is then attached to two rigid substrates to constrain

its stretch as $\lambda_1 = \lambda_p$ in the x-direction. Subsequently, the hydrogel is able to deform in response to acoustic input and temperature variation, obeying the following force balance condition:

$$\sigma_1 = \frac{NkT}{J}(\lambda_1^2 - 1) + \frac{kT}{\Omega}\left[\ln\left(1 - \frac{1}{J}\right) + \frac{1}{J} + \frac{\chi_0 - \chi_1}{J^2} + \frac{2\chi_1}{J^3}\right] - t_1, \tag{5.9}$$

$$0 = \frac{NkT}{J}(\lambda_2^2 - 1) + \frac{kT}{\Omega}\left[\ln\left(1 - \frac{1}{J}\right) + \frac{1}{J} + \frac{\chi_0 - \chi_1}{J^2} + \frac{2\chi_1}{J^3}\right] - t_2 \tag{5.10}$$

and

$$0 = \frac{NkT}{J}(\lambda_3^2 - 1) + \frac{kT}{\Omega}\left[\ln\left(1 - \frac{1}{J}\right) + \frac{1}{J} + \frac{\chi_0 - \chi_1}{J^2} + \frac{2\chi_1}{J^3}\right] - t_3. \tag{5.11}$$

From equations (5.10) and (5.11), stretch λ_2 can be expressed in terms of stretch λ_3, as:

$$\lambda_2 = \frac{1}{2}\frac{\lambda_1\lambda_3}{NkT}(t_2 - t_3) + \frac{1}{2}\sqrt{\left[\frac{\lambda_1\lambda_3}{NkT}(t_2 - t_3)\right]^2 + 4\lambda_3^2}, \tag{5.12}$$

so that the volume ratio $J = \lambda_1\lambda_2\lambda_3$ can be expressed as a function of λ_3. Correspondingly, the normalized acoustic input at a given temperature T can be expressed as:

$$\frac{p_0^2}{\rho_0 c_0^2}\frac{\Omega}{kT} = \frac{1}{t_3}\frac{p_0^2}{\rho_0 c_0^2}\left[\frac{N\Omega}{J}(\lambda_3^2 - 1) + \ln\left(1 - \frac{1}{J}\right) + \frac{1}{J} + \frac{1}{J^2}(A_0 - A_1) + \frac{2}{J^3}A_1 + \left[\frac{1}{J^2}(B_0 - B_1) + \frac{2}{J^3}B_1\right]T\right]. \tag{5.13}$$

Also, the temperature at a given acoustic input takes the form:

$$T = \left\{\frac{\Omega t_3}{kT} - \left[\frac{N\Omega}{J}(\lambda_3^2 - 1) + \ln\left(1 - \frac{1}{J}\right) + \frac{1}{J} + \frac{1}{J^2}(A_0 - A_1) + \frac{2}{J^3}A_1\right]\right\}\left[\frac{1}{J^2}(B_0 - B_1) + \frac{2}{J^3}B_1\right]^{-1}. \tag{5.14}$$

Figure 6*a*,*b* plots the normalized acoustic input as a function of hydrogel stretch and volume ratio at selected temperatures. A succession of equilibrium states of the hydrogel layer is observed. A fixed temperature sets a value of initial stretch, which can be obtained from the interaction between the corresponding curve and the zero acoustic input line. As previously mentioned, the hydrogel has freely swollen to a homogeneous and isotropic state with a free swelling ratio (e.g. $\lambda_p = 202$ at $T = 303$ K). However, as the temperature is increased, the hydrogel shrinks to smaller stretches and volumes, as shown in figure 6. Owing to the nonlinear nature of acousto-thermo-mechanical deformation, the acoustic input versus deformation curves show wavy variation trends. In other words, for given acoustic input and temperature, the hydrogel can be in one or multiple equilibrium states.

Figure 7*a*,*b* plots the variation of temperature as a function of stretch and volume ratio at selected acoustic inputs, respectively, displays a series of equilibrium states of the hydrogel. At zero acoustic input, the temperature versus deformation curve presents a typical thermo-mechanical response of temperature-sensitive hydrogels. Interaction of this zero acoustic input curve with any constant temperature line gives the initial stretch of acoustic actuation at this temperature. The influence of acoustic radiation force can thence be characterized by supposing its quasi-periodic variation on this zero acoustic input curve. Furthermore, as a result of the nonlinear relation between volume ratio J and stretch λ_3, a series of reciprocating knots appear on the temperature versus volume ratio curves of figure 7*b*. The larger the acoustic input, the more and larger the reciprocating knots.

(c) Biaxial constraint

The hydrogel layer can be bi-axially stretched to a prescribed prestretch of $\lambda_1 = \lambda_2 = \lambda_{pre}$ and then attached to a rigid substrate. When this hydrogel layer is submerged in water, its in-plane dimensions cannot change because it has been constrained bi-axially, as shown in figure 1*c*. When subjected to acoustic input and temperature variation, this hydrogel layer undergoes a

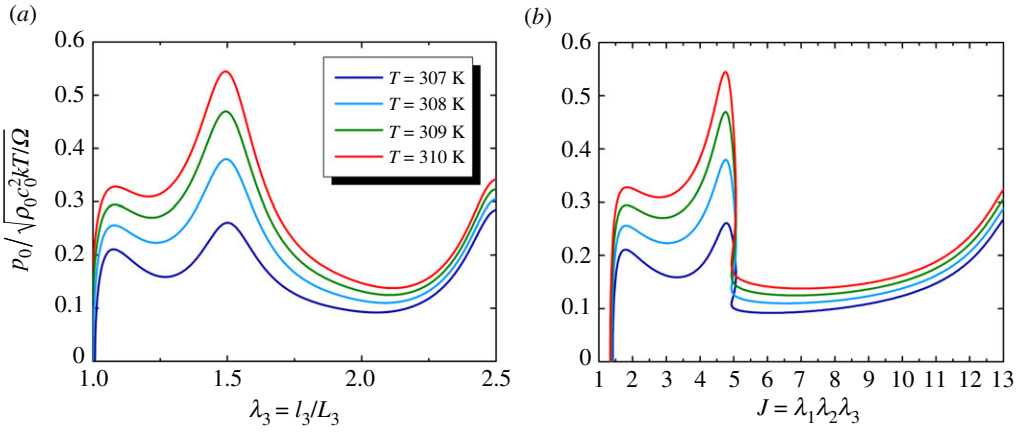

Figure 6. Nonlinear thermo-acousto-mechanical deformation of a uniaxial constrained hydrogel layer under different temperatures: (*a*) acoustic input plotted as a function of out-of-plane stretch and (*b*) acoustic input plotted as a function of volume ratio.

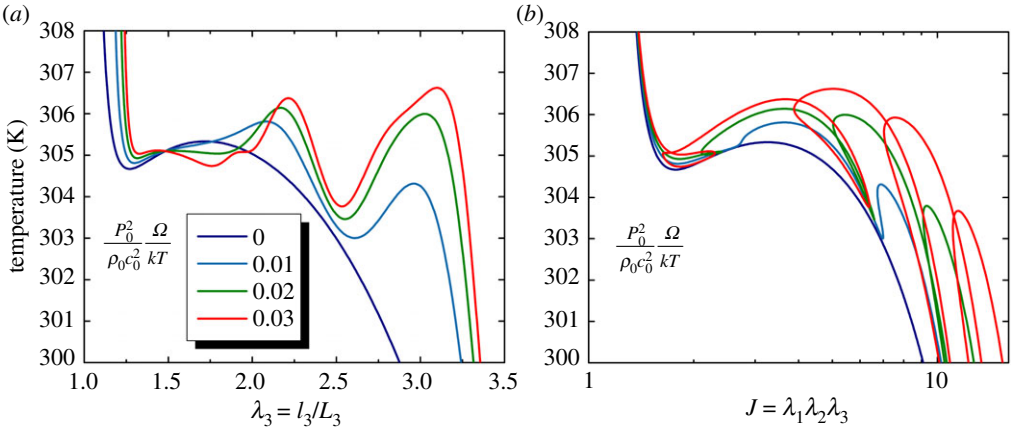

Figure 7. Nonlinear thermo-acousto-mechanical deformation of a uniaxial constrained hydrogel layer at selected acoustic inputs: (*a*) temperature plotted as a function of out-of-plane stretch and (*b*) temperature plotted as a function of volume ratio.

homogeneous and anisotropic deformation along the z-direction and its volume ratio varies as $J = \lambda_{\text{pre}}^2\lambda_3$. Note that the incident acoustic wave penetrating across the hydrogel is totally reflected at the hydrogel–substrate interface. The reflected wave interacts with the incoming wave to generate a standing wave field in the hydrogel layer. Based on this standing wave field, acoustic radiation forces can be calculated. Incorporating these acoustic radiation forces, we write the force balance condition as:

$$\sigma_1 = \frac{NkT}{J}(\lambda_1^2 - 1) + \frac{kT}{\Omega}\left[\ln\left(1 - \frac{1}{J}\right) + \frac{1}{J} + \frac{\chi_0 - \chi_1}{J^2} + \frac{2\chi_1}{J^3}\right] - t_1, \tag{5.15}$$

$$\sigma_2 = \frac{NkT}{J}(\lambda_2^2 - 1) + \frac{kT}{\Omega}\left[\ln\left(1 - \frac{1}{J}\right) + \frac{1}{J} + \frac{\chi_0 - \chi_1}{J^2} + \frac{2\chi_1}{J^3}\right] - t_2 \tag{5.16}$$

and

$$0 = \frac{NkT}{J}(\lambda_3^2 - 1) + \frac{kT}{\Omega}\left[\ln\left(1 - \frac{1}{J}\right) + \frac{1}{J} + \frac{\chi_0 - \chi_1}{J^2} + \frac{2\chi_1}{J^3}\right] - t_3. \tag{5.17}$$

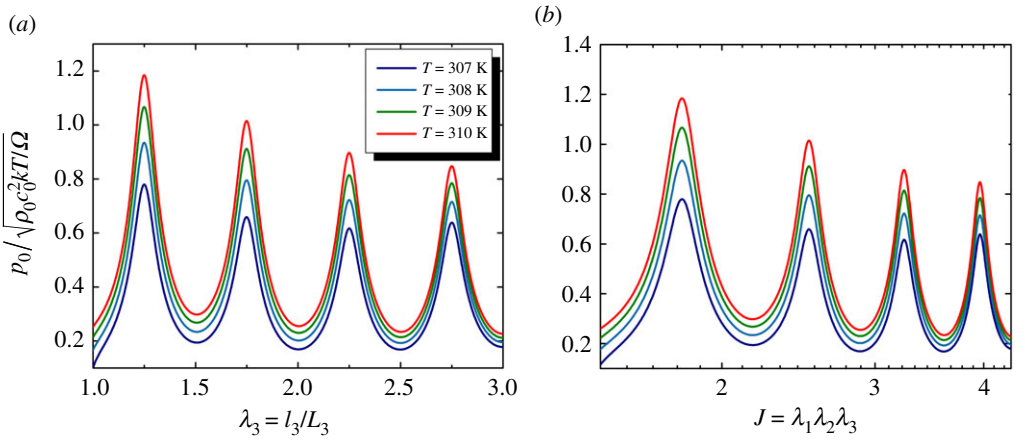

Figure 8. Nonlinear thermo-acousto-mechanical deformation of a bi-axially constrained hydrogel layer under different temperatures: (*a*) acoustic input plotted as a function of out-of-plane stretch and (*b*) acoustic input plotted as a function as a function of volume ratio.

from which we can express the normalized acoustic input as a function of volume ratio at given temperature, as:

$$\frac{p_0^2}{\rho_0 c_0^2}\frac{\Omega}{kT} = \frac{1}{t_3}\frac{p_0^2}{\rho_0 c_0^2}\left[\frac{N\Omega}{J}(\lambda_3^2 - 1) + \ln\left(1 - \frac{1}{J}\right) + \frac{1}{J} + \frac{1}{J^2}(A_0 - A_1) + \frac{2}{J^3}A_1 + \left[\frac{1}{J^2}(B_0 - B_1) + \frac{2}{J^3}B_1\right]T\right]. \tag{5.18}$$

Alternatively, we can express the temperature as a function of volume ratio at given acoustic input, as:

$$T = \left\{\frac{\Omega t_3}{kT} - \left[\frac{N\Omega}{J}(\lambda_3^2 - 1) + \ln\left(1 - \frac{1}{J}\right) + \frac{1}{J} + \frac{1}{J^2}(A_0 - A_1) + \frac{2}{J^3}A_1\right]\right\}\left[\frac{1}{J^2}(B_0 - B_1) + \frac{2}{J^3}B_1\right]^{-1}. \tag{5.19}$$

With the prestretch set at $\lambda_{\text{pre}} = 1.2$, the normalized acoustic input is plotted in figure 8*a*,*b* as a function of stretch and volume ratio for selected temperatures, respectively. As each point on these curves corresponds to an equilibrium state, thus each curve gives a series of equilibrium states of the hydrogel. As only its thickness is allowed to swell under acoustic input and temperature variation, the hydrogel exhibits a relatively regular relationship between normalized acoustic input and stretch/volume ratio. The acoustic input periodically varies with either the stretch or the volume ratio. The larger the temperature, the larger the acoustic input required to maintain the same deformation.

Figure 9*a*,*b* plots separately the temperature as a function of hydrogel stretch and volume ratio at selected acoustic inputs. Again, the role of acoustic radiation force manifests itself when its periodical variation is superposed onto the zero acoustic input curve (as reference). Also, higher temperature corresponds to larger acoustic input. Owing to the nonlinear nature of the present problem, there exist one or multiple stretches related to one given temperature. This phenomenon provides the possibility for multiple phase transitions. Relative to the previous two cases, the temperature versus stretch/volume ratio curves do not exhibit complex reciprocating knots. This is because the strong biaxial constraint leaves only one variable (i.e. λ_3), drastically simplifying the intrinsic nonlinear relation. As the acoustic inputs are increased, the variation of the temperature versus stretch/volume ratio curve becomes larger.

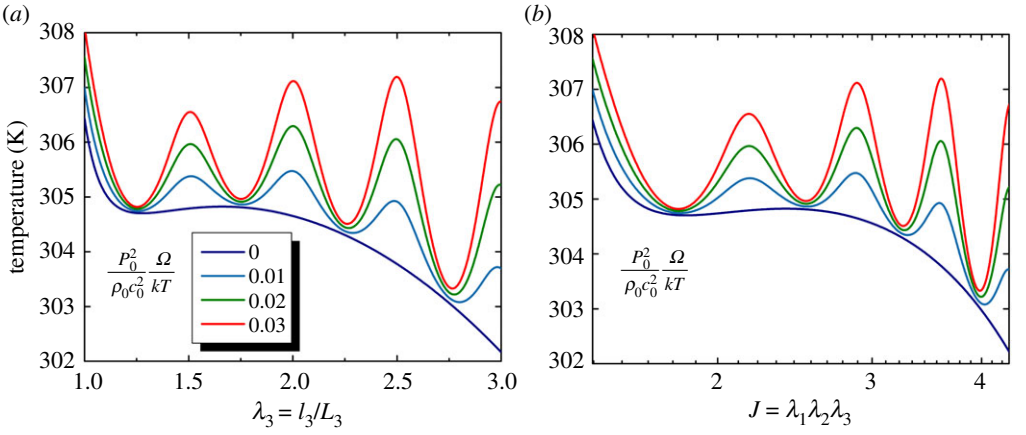

Figure 9. Nonlinear thermo-acousto-mechanical deformation of a bi-axially constrained hydrogel layer at selected acoustic inputs: (*a*) temperature plotted as a function of out-of-plane stretch and (*b*) temperature plotted as a function of volume ratio.

6. Concluding remarks

A nonlinear theory is presented to characterize the large acousto-thermo-mechanical deformation of temperature-sensitive hydrogels immersed in aqueous environment, in which acoustic radiation stress and temperature both contribute to osmotic pressure to cause hydrogel shrinking or swelling. In this theory, the acoustic radiation stress generated by acoustic inputs is a field force and occupies the space both inside and outside the hydrogel, which can thus be regarded as part of material law to response to external mechanical forces. Adopting the Flory–Rehner theory and the acoustic radiation stress theory, we develop the acousto-thermo-mechanical theory by combining the contributions of network stretching, polymers/solvent mixing and acoustic radiation force. Temperature-sensitive behaviour of the hydrogel is accounted for by introducing the temperature-dependent Flory interaction parameter. Theoretical predictions are compared with experimental measurements at zero acoustic input, with good agreement achieved. Using the validated theory, we demonstrate the significant influence of temperature and acoustic input on the variation of hydrogel-free energy. Hydrogel responses to acoustic input and temperature are systematically analysed under free swelling, uniaxial constraint and biaxial constraint, which comprehensively characterize the acoustic-triggered nonlinear deformation behaviour of temperature-sensitive hydrogels with chemical diffusion. Results presented in this study may inspire the design of novel devices, sensors and actuators by manipulating the acoustic-triggered large deformation of temperature-sensitive hydrogels.

Data accessibility. The dataset of 'Appendix A. Acoustic wave propagation and acoustic radiation stress' supporting this article has been uploaded as the electronic supplementary material.

Authors' contributions. F.X.X. conceived the key idea, developed the theoretical model and performed numerical calculations. Both authors contributed to data analyses. F.X.X. wrote the manuscript and both authors approved for publication.

Competing interests. We have no competing interests.

Funding. This work was supported by NSFC (11772248, U1737107 and 11761131003), DFG (ZH15/32-1) and the Shaanxi Foundation for Selected Overseas Chinese (2017025).

Acknowledgements. The authors are grateful to the anonymous referees, whose valuable comments helped to improve the paper.

References

1. Otake K, Inomata H, Konno M, Saito S. 1990 Thermal analysis of the volume phase transition with *N*-isopropylacrylamide gels. *Macromolecules* **23**, 283–289. (doi:10.1021/ma00203a049)

2. Hu Z, Zhang X, Li Y. 1995 Synthesis and application of modulated polymer gels. *Science* **269**, 525–527. (doi:10.1126/science.269.5223.525)
3. Asoh T-A, Matsusaki M, Kaneko T, Akashi M. 2008 Fabrication of temperature-responsive bending hydrogels with a nanostructured gradient. *Adv. Mater.* **20**, 2080–2083. (doi:10.1002/adma.200702727)
4. Suzuki A, Tanaka T. 1990 Phase transition in polymer gels induced by visible light. *Nature* **346**, 345–347. (doi:10.1038/346345a0)
5. Fukunaga A, Urayama K, Takigawa T, Desimone A, Teresi L. 2008 Dynamics of electro-opto-mechanical effects in swollen nematic elastomers. *Macromolecules* **41**, 9389–9396. (doi:10.1021/ma801639j)
6. Drozdov AD. 2015 Swelling of pH-responsive cationic gels: constitutive modeling and structure–property relations. *Int. J. Solids. Struct.* **64–65**, 176–190. (doi:10.1016/j.ijsolstr.2015.03.023)
7. Drozdov AD. 2014 Volume phase transition in thermo-responsive hydrogels: constitutive modeling and structure–property relations. *Acta Mech.* **226**, 1283–1303. (doi:10.1007/s00707-014-1251-9)
8. Xiaoyi CH-HD. 2015 Swelling and instability of a gel annulus. *Acta Mech. Sin.* **31**, 627–636. (doi:10.1007/s10409-015-0496-4)
9. Xin F, Lu TJ. 2017 A nonlinear acoustomechanical field theory of polymeric gels. *Int. J. Solids Struct.* **112**, 133–142. (doi:10.1016/j.ijsolstr.2017.02.013)
10. Randall CL, Gultepe E, Gracias DH. 2012 Self-folding devices and materials for biomedical applications. *Trends Biotechnol.* **30**, 138–146. (doi:10.1016/j.tibtech.2011.06.013)
11. Dong L, Agarwal AK, Beebe DJ, Jiang H. 2006 Adaptive liquid microlenses activated by stimuli-responsive hydrogels. *Nature* **442**, 551–554. (doi:10.1038/nature05024)
12. Jamal M, Zarafshar AM, Gracias DH. 2011 Differentially photo-crosslinked polymers enable self-assembling microfluidics. *Nat. Commun.* **2**, 193–198. (doi:10.1038/ncomms1531)
13. Majidi C. 2013 Soft robotics: a perspective—current trends and prospects for the future. *Soft Rob.* **1**, 5–11. (doi:10.1089/soro.2013.0001)
14. Gibbs JW. 1878 *The scientific papers of J. Willard Gibbs: thermodynamics*. Woodbridge, CT: Ox Bow Press.
15. Biot MA. 1941 General theory of three-dimensional consolidation. *J. Appl. Phys.* **12**, 155–164. (doi:10.1063/1.1712886)
16. Cai GQ, Zhao CG, Sheng DC, Zhou AN. 2014 Formulation of thermo-hydro-mechanical coupling behavior of unsaturated soils based on hybrid mixture theory. *Acta Mech. Sin.* **30**, 559–568. (doi:10.1007/s10409-014-0011-3)
17. Tanaka T, Fillmore DJ. 1979 Kinetics of swelling of gels. *J. Chem. Phys.* **70**, 1214–1218. (doi:10.1063/1.437602)
18. Scherer GW. 1992 Crack-tip stress in gels. *J. Non-Cryst. Solids* **144**, 210–216. (doi:10.1016/S0022-3093(05)80402-8)
19. Baek S, Srinivasa AR. 2004 Diffusion of a fluid through an elastic solid undergoing large deformation. *Int. J. Non-Linear Mech.* **39**, 201–218. (doi:10.1016/S0020-7462(02)00153-1)
20. Hong W, Zhao X, Zhou J, Suo Z. 2008 A theory of coupled diffusion and large deformation in polymeric gels. *J. Mech. Phys. Solid.* **56**, 1779–1793. (doi:10.1016/j.jmps.2007.11.010)
21. Marcombe R, Cai S, Hong W, Zhao X, Lapusta Y, Suo Z. 2010 A theory of constrained swelling of a pH-sensitive hydrogel. *Soft Matter* **6**, 784–793. (doi:10.1039/b917211d)
22. Cai S, Suo Z. 2011 Mechanics and chemical thermodynamics of phase transition in temperature-sensitive hydrogels. *J. Mech. Phys. Solids* **59**, 2259–2278. (doi:10.1016/j.jmps.2011.08.008)
23. Morimoto T, Ashida F. 2015 Temperature-responsive bending of a bilayer gel. *Int. J. Solids Struct.* **56–57**, 20–28. (doi:10.1016/j.ijsolstr.2014.12.009)
24. Mishra P, Hill M, Glynne-Jones P. 2014 Deformation of red blood cells using acoustic radiation forces. *Biomicrofluidics* **8**, 034109. (doi:10.1063/1.4882777)
25. Wijaya FB, Mohapatra AR, Sepehrirahnama S, Lim K-M. 2016 Coupled acoustic-shell model for experimental study of cell stiffness under acoustophoresis. *Microfluid. Nanofluid.* **20**, 69. (doi:10.1007/s10404-016-1734-1)
26. Issenmann B, Nicolas A, Wunenburger R, Manneville S, Delville JP. 2008 Deformation of acoustically transparent fluid interfaces by the acoustic radiation pressure. *EPL* **83**, 34002. (doi:10.1209/0295-5075/83/34002)

27. Walker WF. 1999 Internal deformation of a uniform elastic solid by acoustic radiation force. *J. Acoust. Soc. Am.* **105**, 2508–2518. (doi:10.1121/1.426854)
28. Foresti D, Nabavi M, Klingauf M, Ferrari A, Poulikakos D. 2013 Acoustophoretic contactless transport and handling of matter in air. *Proc. Natl Acad. Sci. USA* **110**, 12 549–12 554. (doi:10.1073/pnas.1301860110)
29. Foresti D, Poulikakos D. 2014 Acoustophoretic contactless elevation, orbital transport and spinning of matter in air. *Phys. Rev. Lett.* **112**, 024301. (doi:10.1103/PhysRevLett.112.024301)
30. Brandt EH. 2001 Acoustic physics: suspended by sound. *Nature* **413**, 474–475. (doi:10.1038/35097192)
31. Xin FX, Lu TJ. 2016 Acoustomechanical constitutive theory for soft materials. *Acta Mech. Sin.* **32**, 828–840. (doi:10.1007/s10409-016-0585-z)
32. Xin F, Lu TJ. 2017 Nonlinear large deformation of acoustomechanical soft materials. *Mech. Mater.* **107**, 71–80. (doi:10.1016/j.mechmat.2017.02.001)
33. Xin FX, Lu TJ. 2016 Acoustomechanical giant deformation of soft elastomers with interpenetrating networks. *Smart Mater. Strtuct.* **25**, 07LT02. (doi:10.1088/0964-1726/25/7/07LT02)
34. Xin F, Lu T. 2016 Tensional acoustomechanical soft metamaterials. *Sci. Rep.* **6**, 27432. (doi:10.1038/srep27432)
35. Xin F, Lu T. 2016 Generalized method to analyze acoustomechanical stability of soft materials. *J. Appl. Mech.* **83**, 071004. (doi:10.1115/1.4033429)
36. Rubinstein M, Colby RH. 2003 *Polymer physics.* New York, NY: Oxford University Press.
37. Afroze F, Nies E, Berghmans H. 2000 Phase transitions in the system poly(*N*-isopropylacrylamide)/water and swelling behaviour of the corresponding networks. *J. Mol. Struct.* **554**, 55–68. (doi:10.1016/S0022-2860(00)00559-7)
38. Oh KS, Oh JS, Choi HS, Bae YC. 1998 Effect of cross-linking density on swelling behavior of NIPA gel particles. *Macromolecules* **31**, 7328–7335. (doi:10.1021/ma971554y)
39. Suzuki A, Sanda K, Omori Y. 1997 Phase transition in strongly stretched polymer gels. *J. Chem. Phys.* **107**, 5179–5185. (doi:10.1063/1.474880)